

Model for Steam Reforming of Ethanol Using a Catalytic Wall Reactor

J.A. Torres^{*1} and D. Montané²

¹Centre Huile Lourde Ouvert et Expérimental (CHLOE) affiliated to the University of Pau, France,

²Department of Chemical Engineering. Rovira i Virgili University. Av Països Catalans, 26. Tarragona, 43007 – Spain

*Corresponding author: CHLOE, UPPA, bâtiment IFR, rue Jules Ferry, BP 27540, 64075 Pau Cédex, France; e-mail: joseantonio.torres@univ-pau.fr

Abstract: Steam Reforming of Ethanol using a novel reactor configuration, called Catalytic Wall Reactor, was successfully studied using COMSOL. COMSOL Multiphysics was selected because is an ideal tool for coupling transport mechanisms (mass, momentum, and heat transfer) with chemical reactions. A mathematical model is used to describe the reactor performance in terms of main variables (concentration and temperature), and dimensionless groups (Nusselt, Sherwood, and Damkohler). Simulations show that CWR maintains a thermal performance adequate for evaluating catalysts under uniform temperature profile. Additionally, CWR performance is affected by mass flow rate and reaction kinetic parameters. CWR presents two zones: one where the axial gradients are influenced by the entrance effects, while in the second the concentration profile is affected mainly because of the extent of the chemical reaction.

Keywords: catalytic wall reactor, steam reforming of ethanol, reaction engineering

1. Introduction

Energy has become a fundamental necessity to guarantee development of the modern society. Among different possible alternatives to produce energy, the system based on Fuel Cells presents two characteristics that make it an attractive option: (i) it augments the overall process efficiency by transforming chemical energy into electricity, through a reduction in the number of low efficiency processes based on mechanical and thermal energy exchange; and (ii) it expands present energy sources because Fuel Cells work with hydrogen, which can be produced from a large variety of feed stocks including fossil and renewable resources (Song 2002).

Recently, researchers have been studying several strategies to supply hydrogen for different kind of Fuel Cells applications. In general, they remark the importance of

developing new reforming technologies at small scale, which must be compact and efficient (Qi, Peppley et al 2007).

Particularly, Steam Reforming of Ethanol (SRE) has been studied recently for H₂ production because it presents several advantages over other chemical reactions (Torres et al, 2007). However, as SRE is an endothermic reaction, it requires a constant heat supply to maintain continuously the operational conditions in the desired temperature range. For endothermic reactions such SRE, both reactor operation under high efficiency conditions and control of the temperature profile along the reactor depend in a large extent on the reactor configuration.

An interesting option to increase efficiency and diminish reactor volume of endothermic reactions such as SRE is based on using multifunctional reactors. The idea is to utilize a device which integrates the chemical reaction with other functions, such as heat transport. Figure 1 represents a comparison between two distinct reactor configurations: a standard Packed Bed Reactor (PBR) and a novel configuration, the Catalytic Wall Reactor (CWR).

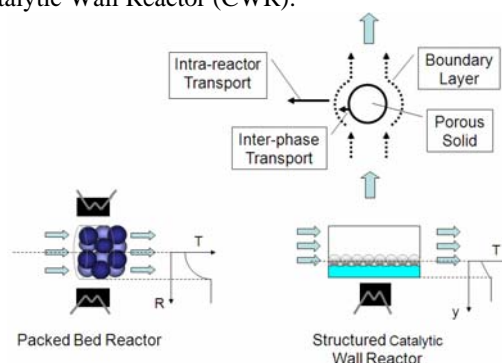


Figure 1. Transport processes (top scheme) are facilitated by arranging catalyst in structures such as catalytic walls (at right-bottom) instead of using disordered configurations like packed bed reactors (at left-bottom).

PBR may present a considerable temperature gradient between the reactor walls and the center. Conversely, in the CWR, the catalyst is deposited on the reactor walls, and is in direct contact with a metallic surface, which is being heated by conduction. As a result, in the CWR configuration the overall process efficiency is incremented by enhancing thermal transfer rates.

This work presents a conceptual analysis using multi-physics simulation for representing a novel Catalytic Wall Reactor configuration. The multi-physics approach is useful to study various coupled physical phenomena, which in the case of heterogeneous catalysis covers mass and heat transport mechanisms coupled with catalytic reaction. The objective of this study is to anticipate possible operational regimes of the CWR unit, constructed to perform catalytic plate tests. COMSOL Multiphysics constitutes a proper option to carry out reactor designing studies because it fulfills the requirement of tackling multiple phenomena, such as mass transport, heat transport, and catalytic chemical reactions.

2. Model

The mathematical model is described and then relevant results are shown, in terms of main variables and main dimensionless groups. The kinetic expression is simplified as much as possible because it is the principal source of uncertainty in the model. Several cases are solved to evaluate sensitivity towards kinetic parameters, such as activation energy and reaction rate constant. Gas phase and solid blocks are studied separately to facilitate the analysis. The mathematical model is based on previous works (Donsi F. et al, 2006; Zafir et al, 2001). Earlier results indicate that in presence of a catalytic wall, the gas channel is affected by development of boundary layers.

2.1 Governing equations

A 2D model is employed for determining concentration and temperature profiles inside the CWR configuration used in the experiments. A complete description of the mathematical model can be encountered elsewhere (Zafir et al, 2001). The catalytic plate is assumed to be adiabatic and symmetric at the centerline of the gas flow channel, as shown on Figure 2.

The model includes: (i) mass and heat balances of the gas phase, through axial convection, conduction, and diffusion in both directions; and (ii) heat balance at the solid block, principally by conduction.

The main assumptions are: steady state, ideal gas behavior, chemical reaction only at the catalytic wall, catalyst layers are thin enough to neglect intra-phase transport, and negligible radiation and pressure drop effects. Finally, diffusion and conduction at reactor outlet are specified to be zero. Continuity equation, mass balance of component j , and energy balance are as follows,

$$\frac{\partial \rho}{\partial t} + \nabla \cdot \rho \mathbf{u} = 0 \quad (1)$$

$$C_0 \left(\frac{\partial y_j}{\partial t} + \mathbf{u} \cdot \nabla y_j \right) = C_0 (D_j \nabla^2 y_j) + \sum_i v_{ij} r_j \quad (2)$$

$$\rho c_p \left(\frac{\partial T}{\partial t} + \mathbf{u} \cdot \nabla T \right) = k_e \nabla^2 T + \sum_i v_{ij} r_j \Delta H_i \quad (3)$$

Analysis of the set of equations (1)-(3) is simplified by grouping several parameters into dimensionless factors, such as Nusselt, Nu , Sherwood, Sh , and Damkholer, Da . These numbers are helpful as a first order estimate for comparing significant influence of the different mechanisms taking place.

2.2 Model parameters

The principal variables of the model are velocity, u , temperature, T , and molar concentration, c . Gas phase is assumed ideal, and the density of the i component, ρ_i , is calculated as,

$$\rho_i = \frac{P}{RT} \frac{1}{\sum \left(\frac{w_i}{MW_i} \right)} \quad (4)$$

where w_i and MW_i are the mass fraction and the molar weight respectively. The mass diffusion coefficient D_j is considered to be a function of temperature,

$$D = D_0 \left(\frac{T}{T_0} \right)^{1.75} \quad (5)$$

where T_0 and D_0 refer to the initial temperature and the diffusion coefficient, respectively.

Thermal properties (heat capacity, c_p , and effective thermal diffusion coefficient, k_e) are considered to remain constant under the conditions studied. Reaction enthalpy, ΔH is computed according to the reaction stoichiometry. Reaction rate, r_j , is assumed to be linearly dependent on the gas phase concentration. Also, reaction rate constant follows the Arrhenius law,

$$-r_j = k_0 \exp\left(\frac{E}{RT}\right) c_j \quad (6)$$

where r_j is the reaction rate of ethanol, k_0 is the reaction rate constant, E is the activation energy, R is the universal constant of gases, and c_j the diffusion coefficient of ethanol in the gas phase.

Table 1 show main factors employed, such as reactor geometry, inlet conditions and kinetic parameters. Geometry and operational conditions are similar to those used in experiments, while uncertain kinetic parameters such as reaction rate constant and activation energy are screened at different levels. Mass flow rate from 0.01 to 1.00 corresponds to Re numbers from 20 to 2000, respectively. Exploration of Re number effects on heat and mass transport is limited to flow rates in the experimental range.

Table 1: Factors used for calculation: reactor geometry, inlet conditions and kinetic parameters

| | | |
|-----------------|-------------------|--|
| Geometry | Channel | 0.2 cm by 2cm by 5cm |
| | Plate | 100cm by 2cm by 5cm |
| Feed conditions | SC | 4 mol _{H2O} /mol _C |
| | T_0 | 773 |
| | Mass flow rate | from 0.01 to 1.00 g min ⁻¹ |
| Linear Kinetic | Reaction rate | from 10 to 10 ⁴ s ⁻¹ |
| | Activation energy | from 64 to 130 kJ mol ⁻¹ |

Finally, initial parameters describing the operational conditions are initial concentration, c_0 , initial velocity, u_0 , and initial velocity, T_0 .

2.3 Dimensionless numbers

Reaction performance was evaluated using three dimensionless groups: Nusselt, Nu ,

Sherwood, Sh , and Damkholer, Da . Each dimensionless group represents a comparison between two different mechanisms: thermal convection-diffusion (Nu), mass convection-diffusion (Sh), and reaction rate-mass diffusion (Da). Employed equations are,

$$Nu = \frac{q}{(T - T_{ave}) k_f} \frac{x}{L} \quad (7)$$

$$Sh = \frac{J}{(C - C_{ave}) D} \frac{x}{L} \quad (8)$$

$$Da = \frac{k_0 \cdot \exp(E/RT) \cdot d_{eq}}{C \cdot D} \quad (9)$$

where u_{ave} , T_{ave} and C_{ave} are the average velocity, temperature and concentration for the gas phase, computed by eqs (10)-(12), q is the local heat rate, J is the local mass flow, x is the axial length, and d_{eq} is a characteristic length, defined as the equivalent diameter for a square channel. Profiles of the three main variables are averaged using following equations,

$$u_{ave} = \frac{\left(\int_0^\delta u \cdot \rho \, dx \right)_{x=L}}{\left(\int_0^\delta \rho \, dx \right)_{x=0}} \quad (10)$$

$$C_{j,ave} = \frac{\left(\int_0^\delta u \cdot C_j \, dx \right)_{x=L}}{\left(\int_0^\delta u \, dx \right)_{x=0}} \quad (11)$$

$$T_{ave} = \frac{\left(\int_0^\delta \rho \cdot c_{p,j} \cdot u \cdot T \, dx \right)_{x=L}}{\left(\int_0^\delta \rho \cdot c_{p,j} \cdot u \, dx \right)_{x=0}} \quad (12)$$

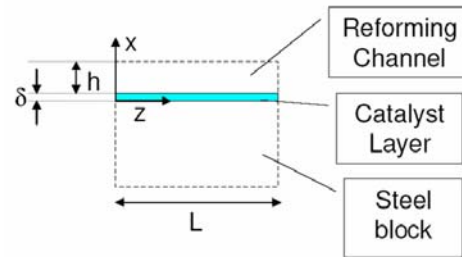


Figure 2. Diagram of studied catalytic plate, an adiabatic reactor with symmetry at the centerline of the channel. The geometry factors are: the catalytic plate thickness δ , the channel thickness h , the block thickness H , and the plate length, L

2.4 Application mode

Four types of application modes were used: (i) convection and diffusion for the mass balance in the gas phase channel, (ii) heat transfer

through convection and conduction for the heat balance in the gas-phase channel, (iii) incompressible Navier-Stokes for momentum balance inside the gas channel, and (iv) heat transfer through conduction for the heat balance in the steel block. The Chemical Engineering Module facilitated the coupling of transport phenomena and chemical reaction kinetics (Comsol, 2007).

3. Results

Figure 3 shows the velocity contour at a mass flow rate of $m=0.1 \text{ g min}^{-1}$. Two marked regions can be observed as a function of the axial position: in the first zone, near the inlet, radial gradients are perturbed by entrance effects while the rest maintains a stable profile in the radial direction. This contour can be related to the development of a momentum boundary layer. Velocity contours are not affected significantly by kinetic parameters, such as frequency factor or activation energy because a system under diluted conditions is considered (i.e. water and carrier gas are in excess compared with ethanol and all the products).

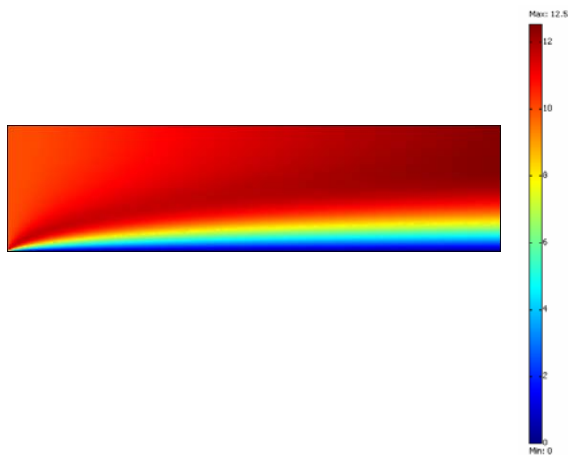


Figure 3. Contour plot for gas phase velocity at mass flow rate of $m=0.1 \text{ g min}^{-1}$. Other models parameters are: $E_a=97 \text{ kJ mol}^{-1}$ and $k_o=100 \text{ s}^{-1}$.

Figure 4 presents contour plots for temperature and ethanol concentration at the flow channel at one level of reaction rate constant ($k_o=100 \text{ s}^{-1}$). Mass flow rate and activation energy are fixed at 1 g min^{-1} and 97 kJ mol^{-1} respectively. Contour plot is adjusted for

comparison purposes by fixing a concentration range, $1.70\text{-}1.75 \text{ mol m}^{-3}$. Temperature is approximately constant (around 773 K).

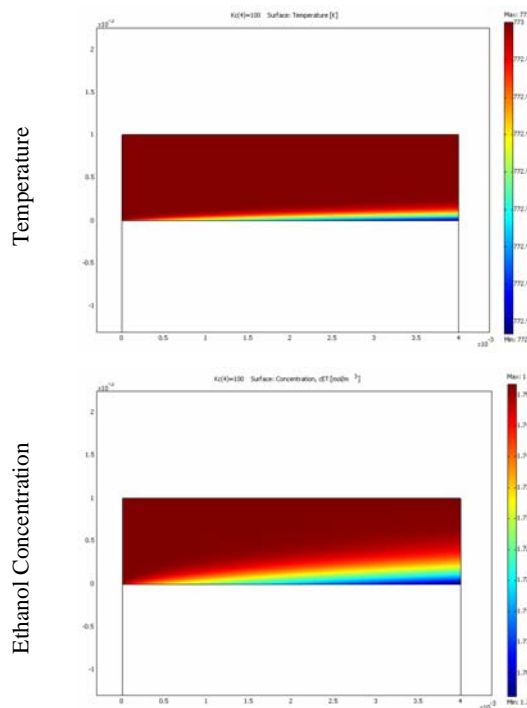


Figure 4. Contour plot for gas phase temperature and concentration under central level of reaction rate constant. Other models parameters are $E_a=97 \text{ kJ mol}^{-1}$ and $m=1 \text{ g min}^{-1}$. Gas phase temperature is approximately 773 K and concentration varies from 1.70 to 1.75 mol m^{-3} .

The concentration gradient between bulk and catalyst surface increases with the axial coordinate because the ethanol consumption augments with reactants residence time. The same dynamics follows for the temperature gradient and the heat consumption. In addition, at higher k_o , the reduction in temperature is higher because the heat demand of the endothermic reaction is proportional to the reaction rate. In general, the temperature contour appears to be isothermal while concentration is progressively affected by axial diffusion and the development boundary layer with high values on the axial coordinate.

Figure 5 presents dimensionless groups Nu , Sh , and Da as a function of the axial coordinate at three levels of mass flow rate from 0.01 to

1.00 g min⁻¹. The reaction rate constant is fixed at 10 s⁻¹ and the activation energy is 97 kJ mol⁻¹.

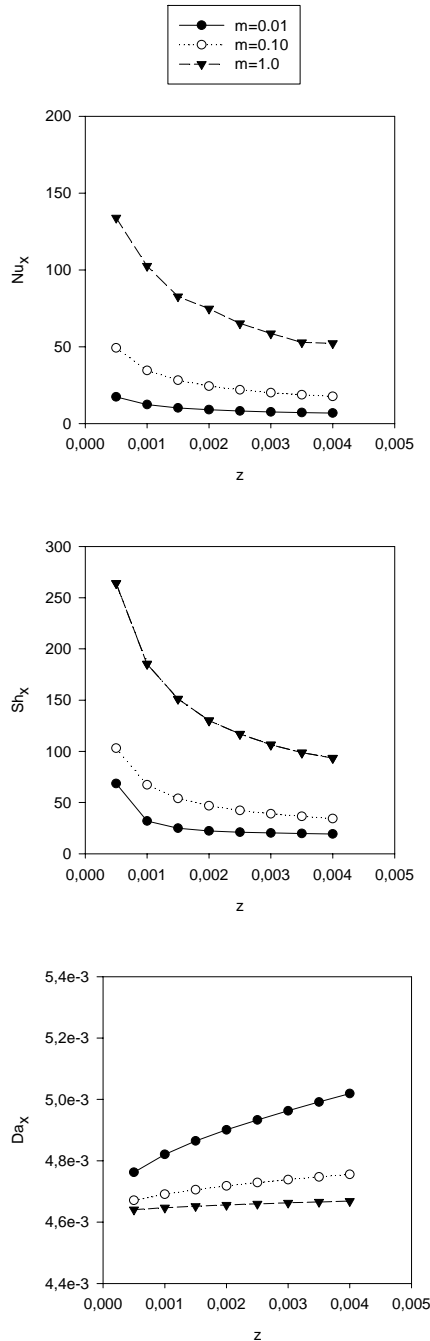


Figure 5. Axial profiles of three different dimensionless groups Nu , Sh , and Da as a function of axial length for three levels of the mass flow rate, from 0.01 to 1.00 g min⁻¹.

Both Nu and Sh numbers present two main regions as a function of axial length, similar to the wall temperature and concentration contours observed in figure 4. A first region, near the inlet, where a marked decline of dimensionless numbers exists. A second region, next to the outlet, where temperature and concentration are almost constant and the dimensionless groups also tend to their asymptotic values. In this zone, Nu and Sh are stabilize around 6.7 and 19.3 respectively, which is in agreement with results for similar problems found in literature (Tronconi et al. 2005; Donsi et al. 2006). On the other hand, Da is approximately $5.0 \cdot 10^{-3}$. Small values of Da indicate that, under these conditions, the CWR system is controlled by the reaction rate (kinetic time is higher than convective time). This circumstance takes place independently of the mass flow rate.

Figure 5 indicates that as the mass flow rate (equivalent to the Re number) is high, the dimensionless groups tends to be shifted; i.e. they will be significantly higher in the overall axial direction. Actually, Sh and Nu at 1.0 g min⁻¹ differ from the asymptotic value at the reactor outlet by multipliers of approximately 1.8 and 2.6, respectively. At higher gas velocities the resistance to axial diffusion increases and major heat and mass fluxes are demanded to sustain the reaction rate.

In summary, gas phase results shows that the CWR performance is affected by mass flow rate and kinetic parameters. The catalytic channel could be divided into two zones, which are characterized by the development of momentum, heat and mass boundary layers. In the first zone, radial gradients are influenced by the entrance effects; while in the second the reaction rate is the principal element that affects radial gradients.

4. Conclusions

The CWR model can be solved using COMSOL Multiphysics. Results showed that at specified conditions CWR maintains a thermal performance adequate for evaluating catalysts under a uniform temperature profile. CWR performance is mainly affected by mass flow rate and reaction kinetic parameters. Future work should focus on obtaining a reliable kinetics for the endothermic SRE reaction to improve numerical predictions and process control.

5. References

1. COMSOL User's Guide, Stockholm, Sweden: Comsol, (2007).
2. Donsi, F., A. Di Benedetto, et al. "Effect of the Re number on heat and mass transport in a catalytic monolith." *Catalysis Today* 117 (4) 498-505. (2006)
3. Qi, A., B. Peppley, K. Karan. "Integrated fuel processors for fuel cell application: A review." *Fuel Processing Technology* 88: 3-22. (2007)
4. Torres, J.A., J. Llorca, A. Casanovas, M. Dominguez, J. Salvado, D. Montané. "Steam reforming of ethanol at moderate temperature: Multifactorial design analysis of Ni/La₂O₃-Al₂O₃, and Fe- and Mn-promoted Co/ZnO catalysts" *Journal of Power Sources*, 169 (1): 158-166. (2007)
5. Tronconi, E., G. Groppi "A study on the thermal behavior of structured plate-type catalysts with metallic supports for gas/solid exothermic reactions." *Chemical Engineering Science* 55 6021-6036. (2005)
6. Song, C. "Fuel processing for low-temperature and high-temperature fuel cells: Challenges, and opportunities for sustainable development in the 21st century" *Catalysis Today*. Volume 77, Issue 1-2, Pages 17-49 (2002)
7. Zafir, M., A. Gariilidis. "Modeling of a catalytic plate reactor for dehydrogenation-combustion coupling." *Chemical Engineering Science* 56 2671-2683. (2001)

6. Acknowledgements

The authors are indebted for financial support to the Spanish Government (project CTQ2005-09182-C02-01/PPQ, partially funded by the FEDER program of the European Union). JA Torres is grateful to CHLOE for supporting his participation in the COMSOL conference. Also, he is thankful to Rovira i Virgili University for providing his PhD scholarship.